CHAPTER 4.0 THE NUMERICAL METHOD

In this chapter, the solution technique used to solve the quasi 2-D Navier-Stokes equations will be described. The discussion will begin with the nature in which the computational space is discretized. MacCormack's method will then be described in detail.

4.1 Discretization

The governing equations are computationally solved in their conservative form, by applying a cell-centered finite difference technique. This involves providing a predetermined number of grid points within the computational space. Since previous numerical approaches utilized less than 20 grid points inside the boundary layer, it was considered ideal to have approximately sixty grid points inside the boundary layer throughout this research. As a result, the total number of grid points in the computational domain could be determined by the boundary layer thickness. This translates to approximately 60 grid points per 0.1mm. Setting the length of the computational domain will provide the total number of grid points required to fill the computational domain. The space between grid points is defined as

$$\Delta y = \frac{L}{(\# gridpo\operatorname{int} s - 1)}$$

where L is the total computational domain length. A uniform grid spacing was used for simplicity.

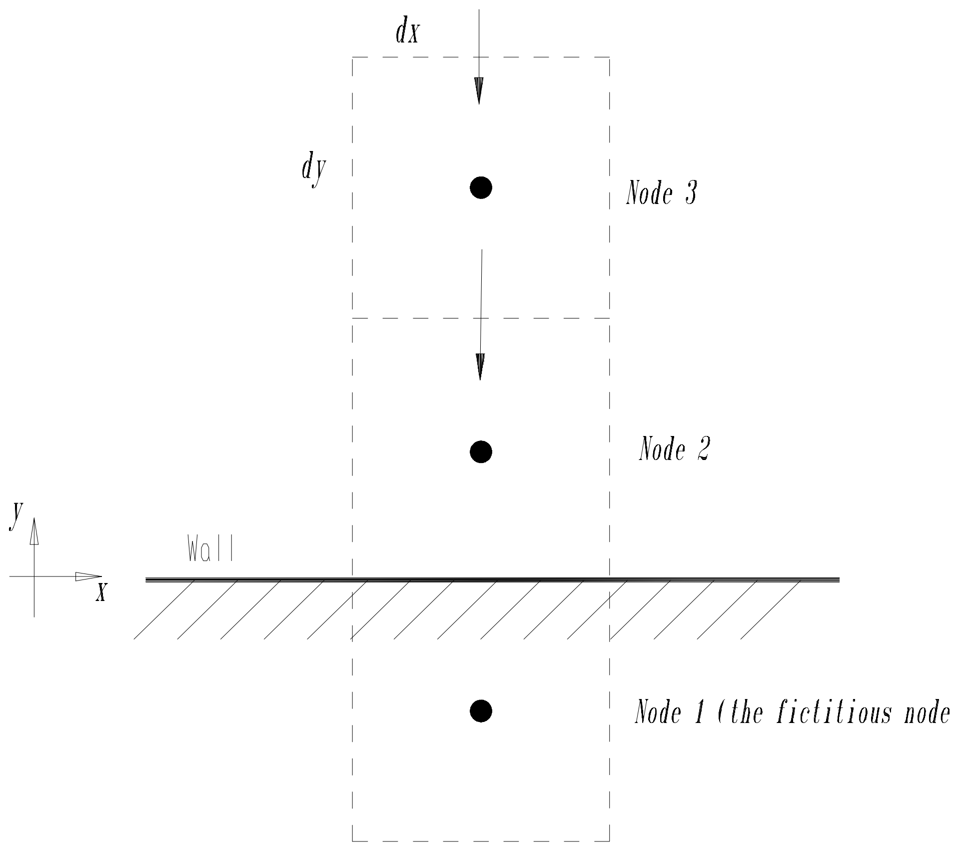

Fig 4.1   Wall nodal points

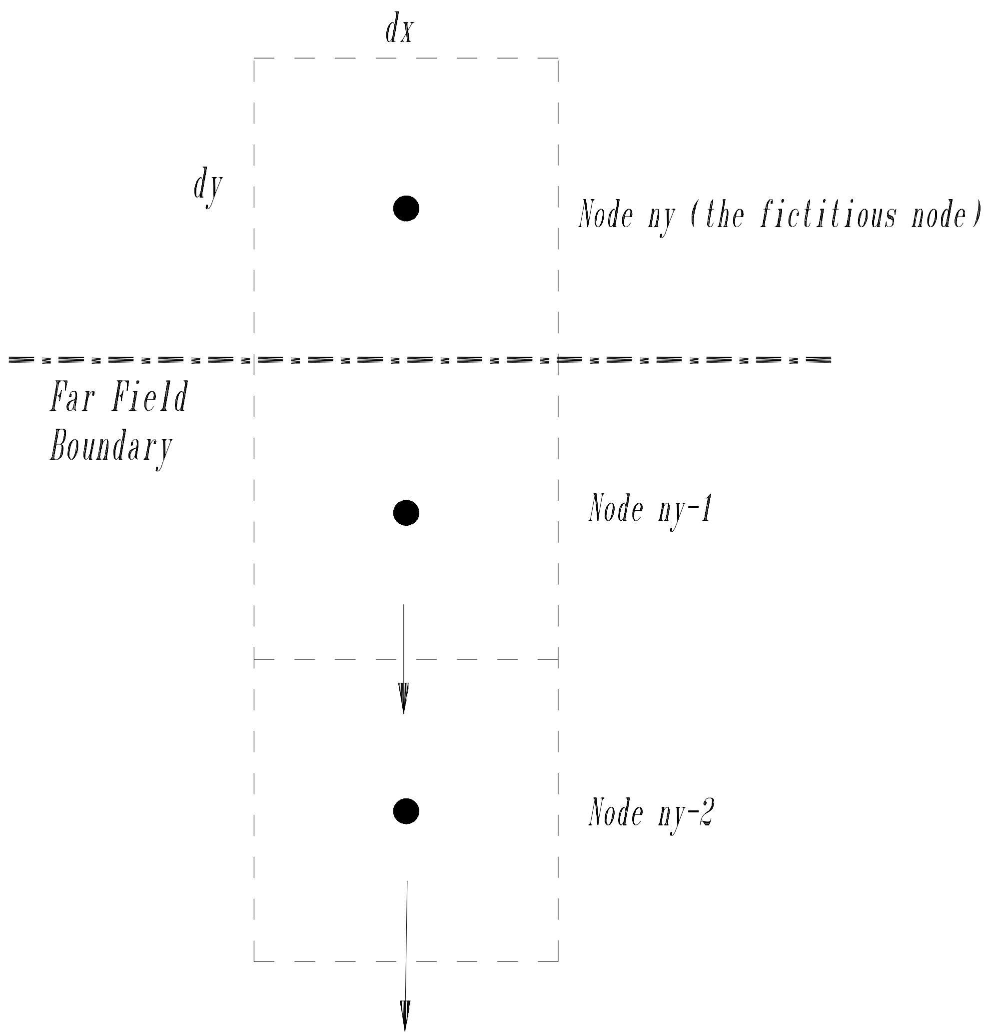

Fig 4.2 Far field nodal points

The grid points are located in the middle of the cell volumes, which are chosen so that the cell boundaries coincide with the wall and the farfield boundaries. This is illustrated in Figures 4.1 and 4.2. Differencing of flow property values at adjacent grid points will produce the flow property fluxes at the cell boundaries. Each of the governing equations corresponds to the conservation of mass, x- and y- momentum, and energy, which are conserved in each of the cell volumes. Applying the finite difference method to the governing equations indicated by equation 3.1 produces

$$\frac{Q_j^{n+1} - Q_j^n}{\Delta t} + \frac{F_{j+1}^n - F_j^n}{\Delta y} = 0 \qquad [4.1]$$

and

$$\frac{Q_j^{n+1} - Q_j^n}{\Delta t} + \frac{F_j^n - F_{j-1}^n}{\Delta y} = 0 \qquad [4.2]$$

Both equations 4.1 and 4.2 are forward and backward finite difference expression, respectively. These representations have an error of magnitude of Δt and Δy, which corresponds to the time step and the distance between adjacent grid points. As long as both are small, the error of these finite difference expressions will be small. These expressions are the basis of MacCormack's method, which will be described in the next section.

4.2 Basic Numerical Approach (MacCormack's Method)

This section briefly describes all of the necessary details required to generate the solution of the governing equations. Similar to an analytical solution of partial differential equations, initial conditions (at time=0) are needed for all of the parameters involved in the equations. This means that the initial flow variable magnitudes (ρ, ρu, ρv, and ρE) at every grid point in the computational space will need to be defined. In addition, the boundary conditions at the blade surface (at x=0) and the farfield boundary (at x=L) will need to be defined. These conditions will be described after discussion of the basic numerical approach.

4.2.1 Dimensions of the Computational Flow Domain

The length of the computational space will determine the maximum total time that this approach will be valid. The flow problem of interest is a shock with a pressure ratio of 1.1. This provides an estimate of the shock velocity before and after impact with the blade surface. The blade surface boundary has a reflective boundary condition. However, since the farfield boundary condition is non-reflecting, the length of the computational space (L) must be chosen so the shock can propagate for a desired length of time after impacting the blade surface. Once the reflected shock impacts the farfield boundary, the computational flowfield becomes unstable and emits nonphysical characteristic values.

The normal shock tables indicate that a shock of strength 1.1 travels at a Mach number of ~1.04. For the flow conditions chosen, the shock can travel a distance of 15mm within 60 μseconds. Therefore, a computational window length of L=15mm was chosen, so that 60 μseconds (maximum) of temperature history would be available after shock impact with the blade surface. For a computational window length of 15mm, the boundary layer only occupies 0.1mm (which is < 1%). This is a drawback created by the slow time scale of heat transfer and has to be tolerated for this analysis. The benefit of using this simplified version of the governing equations is a reduction of the computer time needed to solve this flowfield. The more complicated, full 2-D N-S equations would take considerably longer to produce temperature histories near the wall due to the extra spatial flux vector ($\vec{E}$), which contains additional flow, viscous and heat transfer terms.

At this time, it becomes necessary to decide the number of grid points to be located *inside* the boundary layer. Since a value of 60 was chosen, then the 15mm computational flow space would require a total of 9000 grid points. A reduction of the total number of grid points would reduce the number of grid points inside the boundary layer for the same value of L and Δy. The computational space could have 60 grid points inside of the boundary layer with less than 9000 grid points, but this would correspond to a smaller value of L. A smaller value of L will not produce the 60μsec of time history after shock impact that is desired.

4.2.2 The Numerical Method

MacCormack's 2-step explicit approach is used in this research in the form of

$$\left(Q_{\Pr edictor}\right)_{i,j}^{n+1} = Q_{i,j}^{n} - \frac{\Delta t}{\Delta y}\left(F_{i,j+1}^{n} - F_{i,j}^{n}\right) \qquad [4.3]$$

$$\left(Q_{Corrector}\right)_{i,j}^{n+1} = Q_{i,j}^{n} - \frac{\Delta t}{\Delta y}\left(F_{i,j}^{n} - F_{i,j-1}^{n}\right) \qquad [4.4]$$

$$Q_{i,j}^{n+1} = \frac{1}{2}\left\{\left(Q_{\Pr edictor}\right)_{i,j}^{n+1} + \left(Q_{Corrector}\right)_{i,j}^{n+1}\right\} \qquad [4.5]$$

This method is considered useful for solving vector equations having the form of Equation 3.1. Using the finite difference expressions of Equations 4.1 or 4.2 is unconditionally unstable, which means that with each time step, the error grows unbounded. If a centered-difference scheme is used, then conditional stability is achieved. The stability of MacCormack's predictor/corrector scheme resembles the stability of a centered-difference finite difference scheme, but contains a smaller error term (of order Δt^2 and Δy^2) when compared to Equations 4.1 and 4.2. Past use of MacCormack's method has been proven useful for solving the conservative form of the governing equations with a discontinuity present in the initial conditions.

In Equations 4.3, 4.4, and 4.5, the subscript i equals 1-4 where:

1. Continuity equation
2. X-momentum equation
3. Y-momentum equation
4. Energy equation.

The subscript j is a spatial reference within the computational space. As stated before, a predetermined number of cell volumes containing grid points are established. The computational space is fitted with (ny=) 9000 cell volumes, so that $\Delta y = \frac{L}{9000}$ and y=jΔ y, where the spatial reference j=2-8999. Values of j=1 and 9000 correspond to the blade surface (j=1) and farfield (j=9000) boundary conditions, respectively. The subscript n is a time level reference, where n=0 corresponds to the initial values of the flow field variables.

Boundary condition limitations require that the calculations terminate prior to the reflected shock impacting the far field boundary. Once the total time is estimated, the stability criteria of MacCormack's method will dictate the size of the time step Δt. When this time step is determined, the total number of steps can be obtained. This provides the maximum time that the calculated solutions to the governing equations. This is determined from $t=n\Delta t$. It is recommended to advance in time with as big a time step as possible which makes knowing the maximum allowable time step crucial.

4.2.3 Maximum Allowable Time Steps

The interval and total number of time steps depend on the computational domain dimensions and properties. Tannehill[26] has empirically determined the time step for this method. The relation defining the maximum allowable time step is

$$\Delta t \leq \frac{\sigma(\Delta t)_{CFL}}{1+\frac{2}{\mathrm{Re}_{\Delta}}} \qquad [4.6]$$

In equation 4.6, σ is a safety factor $\cong 0.9$ (recommended), and $(\Delta t)_{CFL}$ is the inviscid CFL condition, defined as

$$(\Delta t)_{CFL} \leq \frac{\Delta y}{|a|+v} \qquad [4.7]$$

The minimum mesh Reynolds number Re_{Δ} is given by

$$\mathrm{Re}_{\Delta} = \frac{\rho|v|\Delta y}{\mu} \qquad [4.8]$$

According to Anderson[27], the grid Reynolds number for a perpendicular distance away from a flat plate should be $\leq$ 3-4. Using these relations, the maximum time step used was approximately 90% of those calculated from Equation 4.6.

4.2.4 Application of MacCormack's Method

As recommended by Hirsch[28], the forward difference predictor/backward difference corrector application of MacCormack's 2-step method would best approximate a flow field that has a shock propagating toward the bottom of the computational window. This scenario corresponds to an incident shock approaching a plane wall, which is located at the bottom of the window. The backward difference predictor/forward difference corrector application of MacCormack's 2-step method would best approximate a flow field that has a shock propagating toward the top of the computational window. This scenario corresponds to a reflected shock propagating away from a plane wall, which is located at the bottom of the window. The physical problem under investigation contains both an incident and reflected shock wave. For this reason, the numerical approach will include alternating the predictor/corrector sequence to resolve the best solution for a shock moving in either direction. The alternating sequence utilized becomes:

1. Forward difference predictor/Backward difference corrector (on odd time levels: n is odd)
2. Backward difference predictor/Forward difference corrector (at even time levels: n is even).

This alternating sequence is felt to be an important step in the calculation of a flow field consisting of shocks moving in either direction. If a forward difference predictor/backward difference corrector is used exclusively, the incident shock is captured nicely but the reflected shock is not captured very well. The same thing occurs for the reflected shock if a backward difference predictor/forward difference corrector is used exclusively. Because of this, the alternating sequence is applied to all steps, and reasonable shock resolution is maintained for both incident and reflected shocks.

4.3 Boundary Conditions

The final elements needed to begin the solution of the governing equations are the boundary conditions. This problem contains 2 distinct boundaries, one at the blade surface and the other at the farfield, shown in Figures 4.1 and 4.2.

Figure 4.1 illustrates that the nodal point numbering begins at the wall. Two options were available for establishing the wall boundary conditions. They are referred to by Roach[29] as the 1st and 2nd mesh systems. The 1st mesh system is suitable for the Euler equations and involves placing a nodal point on the wall, with other nodal points placed uniformly above at distances that are multiples of dy. However, Roach found it to generate significant errors when applied to the Navier-Stokes equations. The 2nd mesh system, which is used throughout this investigation, is more suitable for this body of research. Nodal points straddle the wall and are averaged to maintain the necessary wall conditions. Roach suggested that it would be more convenient to use the 1st mesh system in the absence of a shock. However, shock reflection is a major element of the problem and reflective boundary conditions are more accurately implemented in the 2nd mesh system. The 2nd mesh system reflective boundary conditions at the blade surface are

$$\left.\frac{\partial \rho}{\partial y}\right|_{wall} = 0 \qquad \text{or} \qquad \rho_1 = \rho_2$$

$$u_{wall} = \frac{u_1 + u_2}{2} = 0 \qquad \text{or} \qquad u_1 = -u_2$$

$$\left.\frac{\partial v}{\partial y}\right|_{wall} = 0 \qquad \text{or} \qquad v_1 = v_2$$

$$\left.\frac{\partial P}{\partial y}\right|_{wall} = 0 \qquad \text{or} \qquad P_1 = P_2$$

$$T_{wall} = \frac{T_1 + T_2}{2} = 300\ \text{K} \qquad \text{or} \qquad T_1 = 2T_{wall} - T_2$$

These conditions enable the wall conditions to be maintained by varying the fictitious node point (node 1). Simply stated, node point 1 is a function of the wall conditions and node point 2.

The farfield boundary is approached in the same manner. Similar to the wall boundary, the far field boundary is evaluated by means of the 2nd mesh system, shown in Figure 3.9. The farfield boundary conditions do not contain the reflective conditions. As a result, the distance L (distance between wall and far field boundary) dictates the length of time for which the approach applies. As stated before, the maximum time for the consecutive calculation of the governing equations should not exceed the time required for the reflected shock to impact the far field boundary. The far field boundary (FFB) conditions stipulate that the flow variable fluxes are zero. This is shown below as

$$\left.\frac{\partial \rho}{\partial y}\right|_{FFB} = 0 \qquad \text{or} \qquad \rho_{ny} = \rho_{ny-1}$$

$$\left.\frac{\partial u}{\partial y}\right|_{FFB} = 0 \qquad \text{or} \qquad u_{ny} = u_{ny-1}$$

$$\left.\frac{\partial v}{\partial y}\right|_{FFB} = 0 \qquad \text{or} \qquad v_{ny} = v_{ny-1}$$

$$\left.\frac{\partial P}{\partial y}\right|_{FFB} = 0 \qquad \text{or} \qquad P_{ny} = P_{ny-1}$$

$$\left.\frac{\partial T}{\partial y}\right|_{FFB} = 0 \qquad \text{or} \qquad T_{ny} = T_{ny-1}$$

Just like the wall boundary conditions, the far field boundary conditions enable the properties at the far field boundary to be maintained by varying the fictitious node point (node ny). Simply stated, the fictitious node point ny is a function of the far field conditions and node point ny-1. In summary, MacCormack's method is used to advance the main flow variables in time (node points 2-8999), and then the fictitious points (node points 1 and 9000) are updated to maintain the predetermined values at the boundaries.

This concludes the description of the numerical method. This method will be tested with less complicated governing equations applied to less complicated experimental data. These test examples will be described in the next chapter.